J. Membrane Biol. 78, 235–248 (1984)

The Journal of
Membrane Biology

Slow Potential Changes in Mammalian Muscle Fibers during Prolonged Hyperpolarization: Transport Number Effects and Chloride Depletion

Peter H. Barry and Angela F. Dulhunty

Nerve-Muscle Research Centre, School of Physiology and Pharmacology, University of New South Wales, Kensington, New South Wales, 2033, and Department of Anatomy, University of Sydney, New South Wales, 2006 Australia

Summary. Mammalian skeletal muscle fibers exhibit large slow changes in membrane potential when hyperpolarized in standard chloride solutions. These large slow potential changes are radically reduced in low chloride solutions, where the faster and smaller potential change ("creep"), usually observed in amphibian fibers, becomes apparent. The slow potential change during a hyperpolarizing current pulse leads to an increase in apparent resistance of up to nine times the instantaneous value and takes minutes to reach a steady value. It then takes a similar time to decay very slowly back to the resting membrane potential after the current pulse. The halftime for the slow potential change was found to be inversely proportional to the current magnitude. From measurements of immediate post-pulse membrane potentials, assuming constant ionic permeabilities, the internal chloride concentration was calculated to decrease exponentially towards a steady value (e.g., for one fiber from 12.3 to 6.6 mM after a 330-sec pulse). The time course and magnitude of the concentration change were predicted from chloride transport number differences, and the known and measured properties of the fibers, and were found to agree very well with the values obtained from experimental measurements. In addition, the shapes of the $V_2 - V_1$ responses, measured in the three-electrode current clamp set-up with either potassium chloride or potassium citrate current electrodes, were as predicted by transport number chloride depletion effects and were at variance with the predictions of a permeability change mechanism.

Key Words transport number effects · chloride depletion · slow potential changes · slow conductance changes · creep · mammalian muscle

Introduction

Mammalian skeletal muscle fibers are known to differ from amphibian fibers in at least two significant ways. Mammalian fibers have an active chloride pump so that the internal chloride ion concentration is not in equilibrium with the resting membrane potential as it is in amphibian fibers (Dulhunty, 1978). In addition, the chloride permeability, which is a significant fraction of the total membrane permeability, is distributed over the surface and T-tubule membranes (Dulhunty, 1979), in contrast to amphibian fibers where chloride permeability is confined to the surface membrane (Eisenberg & Gage, 1969). With these differences in mind, we have examined the response of mammalian muscle fibers to long hyperpolarizing current pulses.

It has been known for some time that hyperpolarizing currents applied across the membrane of amphibian skeletal muscle fibers result in slow potential changes, which appear to reflect increases in membrane resistance and which are colloquially referred to as conductance or resistance "creep" (e.g., Adrian & Freygang, 1962), and which have two potential dependent components (Almers, 1972*a*, *b*). Following hyperpolarizations of less than 30 mV, the potential recovers slowly with a Q_{10} of about 1.3, consistent with a diffusion process, whereas for much larger hyperpolarizations there is a dominating component which is much more temperature sensitive, having Q_{10}'s of 3.0 and 2.8 for the rate of increase of creep itself and for the rate of recovery after the pulse. The former low Q_{10} component is therefore considered to be due to potassium depletion within the transverse tubular system of the muscle fibers. It was further shown (Barry & Adrian, 1973) that for this component the actual time-dependent changes in membrane potential were to be expected from transport number considerations and could be accurately predicted from muscle fiber parameters and known geometry factors. The second component, with a higher Q_{10} and faster recovery, was shown to be consistent with a time and voltage-dependent membrane permeability change (Almers, 1972*b*). The above effects were most clearly

seen when chloride ions were replaced by sulphate ions in the external solution. In such cases the average time constants for small (less than 30 mV) constant voltage and constant current pulses were respectively 400 and 500 msec, the final decreases in conductance also being respectively 0.56 and 0.70 of the initial value (Barry & Adrian, 1973), the effects being very considerably reduced in the presence of normal chloride concentration.

The results in this paper will show that similar slow potential changes are seen in mammalian muscle fibers in solutions with a low chloride concentration. However, in marked contrast to amphibian fibers, when mammalian fibers are hyperpolarized in the presence of standard chloride concentrations there is an even larger and slower potential change, which reaches a maximum value over a period of minutes. Since the ratio of chloride to potassium permeability, P_{Cl}/P_K, is high (in rat sternomastoid fibers $P_{Cl}/P_K = 4.5$; Dulhunty, 1979), the large slow potential change must reflect either a slow change in chloride permeability or a change in the internal chloride concentration.

Analysis of this phenomenon suggests that it is due to the changes in internal chloride concentration within the main intracellular compartment of the muscle fibers, which arise as a result of transport number effects. A preliminary report of some of the material in this paper has appeared elsewhere (Barry & Dulhunty, 1983).

Materials and Methods

The experiments were performed on the surface fibers of small bundles of rat white sternomastoid fibers that had been fine-dissected so that the ends of the fibers were clearly visible. The preparations were mounted in a perspex bath, which was surrounded by a temperature-controlled water jacket. The bathing solution was not flowed during electrical measurements in order to reduce flow artifacts. The external solutions used are listed in Table 1. Experiments were done at 17–23 °C in order to minimize activity of the active chloride pump. Temperature was not lowered below 17 °C because chloride permeability is considered to be reduced at low temperatures (Palade & Barchi, 1977). In all cases the internal and external microelectrodes were filled with 3 M KCl and had resistances of 2–6 MΩ except in those experiments considered for Fig. 10, in which the chloride in the current electrode was replaced by citrate. Chart records of voltage and current traces were obtained on a Hewlett Packard 7401 pen recorder.

A three microelectrode current clamp at the end of the muscle fiber (*see* inset to Fig. 1) was used in order to get a reasonably constant and uniform current density in that region. The space constant of the fiber λ was obtained using a numerical iterative procedure from the exact equation (Adrian, Chandler & Hodgkin, 1970; Barry & Adrian, 1973)

$$\frac{\cosh(2\ell/\lambda)}{\cosh(\ell/\lambda)} = \frac{V_2}{V_1} \tag{1}$$

having used the following approximate expression to obtain an initial value:

$$\frac{V_2 - V_1}{V_1} = \frac{3}{2}(\ell/\lambda)^2 \tag{2}$$

where V_1 and V_2 refer to the voltages measured at the positions ℓ and 2ℓ shown in the inset to Fig. 1. r_i the resistance per unit length was calculated from

$$r_i = V_1 \frac{\exp[(2\ell + \lambda)/\lambda]}{I_0 \cosh(\ell/\lambda)} \tag{3}$$

where I_0 is the total current applied through the current electrode.

The fiber radius a and the membrane current per unit area I_m (at $x = \lambda$) were obtained from the equations

$$a = [R_i/\pi r_i]^{1/2} \tag{4}$$

$$I_m = \frac{a(V_2 - V_1)\cosh(\ell/\lambda)}{2R_i\lambda^2\left[\cosh\left(\frac{2\ell}{\lambda}\right) - \cosh\left(\frac{\ell}{\lambda}\right)\right]} \tag{5}$$

where R_i is the internal resistivity of the fiber. This was assumed to have the value of 169 Ω cm at 20 °C. This value is the same as that determined by Hodgkin and Nakajima (1972) for amphibian fibers and has been shown to be appropriate for mammalian fibers because it gives calculated diameters that are similar to measured diameters in sternomastoid fibers (Davey, Dulhunty & Fatkin, 1980). It was corrected for the particular temperature, using a Q_{10} value of 1.37, from the relationship

$$\frac{R_i(T)}{R_i(T + \Delta T)} = \exp\left[\frac{\Delta T(T + 10)}{10(T + \Delta T)} \ln Q_{10}\right] \tag{6}$$

where $R_i(T)$ is the value at temperature T in °K and $R_i(T + \Delta T)$ its value at temperature $T + \Delta T$.

All calculations and numerical analyses were done using an LSI 11/02 computer (Digital Equipment Corporation).

Results

Experiments were performed on 40 fibers from 15 animals, and essentially similar results were obtained in each case. A few fibers were held for periods exceeding 1 hr with little or no decrement in the resting membrane potential, and the results from these fibers were used to compare experimental results with theoretical predictions.

Figure 1 shows the typical response obtained for a hyperpolarizing pulse across the membrane of a mammalian muscle fiber bathed in one of the two standard chloride Kreb's so-

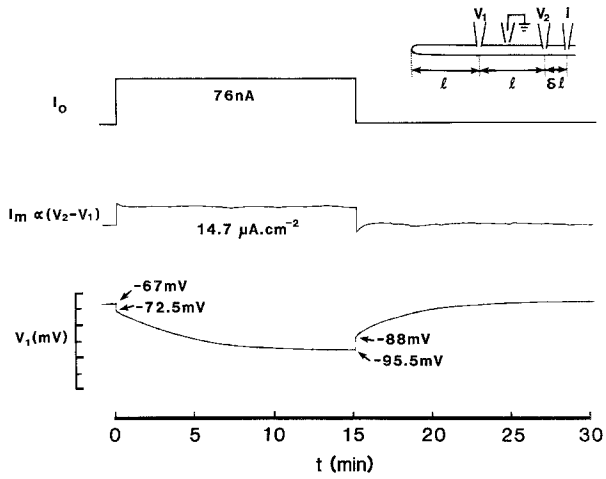

Fig. 1. Slow time-dependent potential changes observed in mammalian muscle fibers in standard Cl solutions (Solution *A* of Table 1). This was measured using the three microelectrode end-of-fiber current clamp setup depicted in the top inset, where *I* represents the current electrode and V_1 and V_2 the voltage recording electrodes. The setup with interelectrode distances ℓ and $\delta\ell$ was designed to give a reasonably constant current density in the end-of-fiber region. In this and in the subsequent figures showing current and voltage records, the top trace, I_o, was drawn in to represent the duration, timing, and shape of the total clamp current in the hyperpolarizing direction, whereas the other traces were reproduced from the original chart records. The bottom trace V_1 in the main panel of this figure shows the initial resistive voltage "jump," in this case from −67 to −72.5 mV. This is then followed by the long slow "creep" towards a steady level, the immediate "jump" at the end of the pulse (in this case, from −95.5 to −88 mV) and the slow recovery or repolarization phase back to the original resting level. The middle trace shows the voltage difference between the V_2 and V_1 electrodes and is proportional to the membrane current density I_m. From this and other measurements the current density in this pulse and the fiber radius were calculated to be 14.7 $\mu A \cdot cm^{-2}$ and 32 μm, respectively, using Eqs. (1)-(6). The interelectrode distances ℓ and $\delta\ell$ were 470 and 94 μm, respectively, resistance $R_m = 0.345\,k\Omega \cdot cm^2$ and the temperature $T = 22\,°C$. Note the small overshoot and undershoot at the beginning and end of the pulse

lutions (Solution *A*, Table 1), using the three microelectrode end-of-fiber current clamp setup illustrated in the inset. The initial resting membrane potential V_m measured by V_1 in this example is −67 mV. During the onset of the current there is a voltage jump followed by a slow increase in membrane potential to a more hyperpolarized level (in this case −95.5 mV). Such an increase in membrane potential, which appears to reflect an increase in resistance, is often referred to as resistance "creep." At the end of the pulse the voltage immediately jumps to an intermediate value (e.g., −88 mV) and then slowly, over about 10 min, returns to its original value.

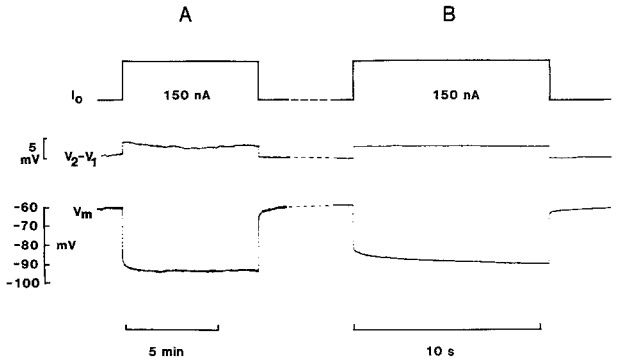

Fig. 2. Voltage responses for two constant hyperpolarizing pulses in a low chloride solution (solution *C* of Table 1) measured using the three-microelectrode current clamp setup (Fig. 1, inset). The two lower traces in both *A* and *B* give the voltage difference $(V_2 - V_1)$, which is considered to be proportional to the membrane current, and the membrane potential V_m, measured as V_1. The two top traces give the total clamp current I_o injected into the fiber in each case. Note that the set of records in *A* has a time course comparable to that of Fig. 1, whereas that in *B* was recorded at a very fast chart speed (60× faster). Because of the lack of Cl (only about 16% of that used in the experiment shown in Fig. 1) and reduction in chloride conductance there is a much greater immediate change in membrane potential at the onset and turn off of the current pulse. In addition the slow time-dependent potential changes are very significantly decreased. There is, however, a faster potential change component similar to that seen in amphibian muscle fibers in low chloride solutions and demonstrated to be due to transport number depletion of K^+ ions in the transverse tubular system of those fibers. From these and other measurements the current density in these pulses and the fiber radius were calculated to be 18.8 $\mu A \cdot cm^{-2}$ and 46 μm, respectively. The interelectrode distances ℓ and $\delta\ell$ were 400 and 200 μm, respectively, membrane resistance was 1.28 $k\Omega\,cm^2$ and $T = 22.6\,°C$

In contrast, when the external chloride is reduced to about 16% of its standard concentration (Solution *C*, Table 1) there is a radical decrease in the amplitude of the slow change in membrane potential (Fig. 2*A*). In addition, there is an increase in the amplitude of the immediate voltage jump when this is compared with the values obtained in standard chloride solutions (*see* Fig. 1). This increase presumably occurs because of the increased membrane resistance in the absence of the normally high chloride conductance. The faster potential changes seen in Fig. 2*B*, occur because the low external chloride concentration has unmasked the relatively faster component of the potential change due to a transport number depletion of potassium ions within the transverse tubular system, as observed in amphibian skeletal muscle especially in the presence of low chloride (Adrian & Freygang, 1962; Almers, 1972*a*, *b*; Barry & Adrian, 1973).

Table 1. Ionic composition of solutions in mM

Solution[a]	Na^+	K^+	Cl^-	NO_3^-	HCO_3^-	Ca^{++}	Mg^{++}	Co^{++}
A	150	3.5	160.5	-	-	2.5	1.0	-
B	145	3.5	150.5	-	25	2.5	1.0	10
C	145	3.5	28.5	147.0	-	2.5	1.0	10
D	145	3.5	153.5	-	-	2.5	1.0	10

[a] In addition all solutions contained 11.0 mM glucose, TTX at 10^{-7} g · ml^{-1} and 2.0 mM TES (N-tris-(hydroxymethyl)-methyl-2-amino-ethanesulphonic acid) buffer at pH 7.4. Solution *D* also contained 25 mM methyl sulphate.

These results immediately suggest that the large slow potential change is due to the presence of chloride ions. The response during the current could either be due to a time-dependent change in: (1) the membrane chloride conductance; (2) P_{Cl}/P_K or (3) the relative concentration of chloride ions outside and inside the cell $[Cl]_o/[Cl]_i$. The shift in potential immediately following the current pulse and its slow recovery back to the original resting potential suggests either that there has been a very slow time-dependent recovery of a permeability change induced by the current pulse or that there was a radical change in the chloride concentration ratio as a result of the current pulse, the most likely mechanism being a change in the chloride concentration within the cell. We will now show that the slow potential change can be predicted from the known properties of the fibers without having to invoke any time or voltage dependence of the ionic permeabilites.

Figures 3 and 4 show a series of voltage responses recorded from one cell as the amplitude of current pulses was increased. Two broad conclusions may be drawn from the results shown in these two figures. Firstly, the rate of change of voltage with time dV/dt increases as the current is increased. Secondly, the membrane potential immediately after the termination of the current pulse (the "immediate post-pulse potential") remains fairly constant and fairly independent of the magnitude of the currents. The increase of dV/dt with current can readily be seen if the time $t_{1/2}$, taken for the voltage change to reach half its maximum value (*see* inset to Fig. 5), is plotted against the magnitude of the current. This is done in Fig. 5, where it can be seen that $t_{1/2}$ decreases linearly with I_m. This simple inverse relationship could be easily be explained in terms of a fixed amount of chloride that needs to be depleted by the current before a steady-state situation is reached.

It should be noted that any changes in chloride concentration within the fiber would tend to affect the voltage response in two ways: (1) by changing the diffusion potential component and (2) by actually changing the chloride conductance through the membrane. In order to investigate the first mechanism, fibers were subjected to a series of hyperpolarizing current pulses of equal magnitude but with different durations, varying from 5 to 330 sec. In order to ensure starting conditions as close as possible to each other a series of pulses, recorded from one fiber in which the initial resting potentials before each pulse were within 1 mV, was chosen for analysis as indicated in Fig. 6. The im-

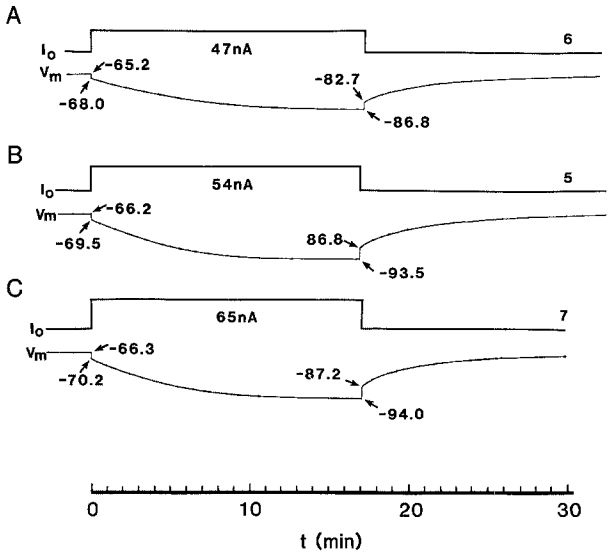

Fig. 3. Slow time-dependent potential changes observed in the same mammalian muscle fiber in a standard Cl solution (Solution *A* of Table 1) for three different values of hyperpolarizing current. This was the same fiber as that used for Fig. 1 with the same parameters and experimental conditions. In each case the lower trace is V_m (measured at V_1), and I_o represents the total current (with its value shown in nA). Note the slight increase in the immediate post pulse potential (following the voltage jump at the end of each current pulse) as the current is increased from *A* to *B* and the slight decrease in the time taken for a steady-state level in V_m to be reduced during the current pulse. The second number above and to the right of the current traces gives the position in the pulse sequence

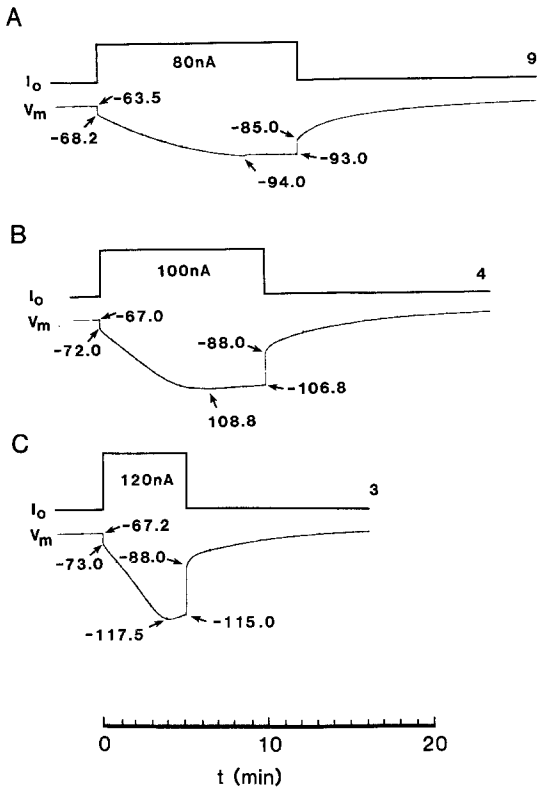

Fig. 4. Slow time-dependent potential changes observed in the same mammalian muscle fiber and conditions as Fig. 3 (and Fig. 1) for three much greater values of hyperpolarizing current. Note the radical decrease in time taken for the voltage response to reach a steady level as the magnitude of the current is increased. In contrast, from *B* of Fig. 3 to *C* of this figure there is very little change in the immediate post pulse potential. These observations are consistent with a transport number depletion of a fixed quantity of chloride from within the fiber down towards a certain fixed concentration level

mediate post-pulse potentials $V(t_3)$ (*see* inset to Fig. 7) were then measured and were used to calculate the internal chloride concentration at the end of the pulse. The immediate post-pulse potentials were considered to reflect the diffusional component of the membrane potential at different times after the onset of the current. The procedure used was as follows: from the initial resting membrane potential $V_m(V(t_o)$ (*see* inset to Fig. 7), using internal potassium and sodium concentrations, $[K]_i$ and $[Na]_i$, of 157 and 60 mM, a P_{Cl}/P_K of 4.5 (Lipicky & Bryant, 1966; Dulhunty, 1978), and P_{Na}/P_K, the ratio of sodium to potassium permeability, of 0.008 (Dulhunty, 1978), a value for internal chloride concentration, $[Cl]_i$, was calculated from the Goldman-Hodgkin-Katz Equation (Goldman, 1943; Hodgkin & Katz, 1949), which has been shown to fit mammalian muscle data (Dulhunty, 1978)

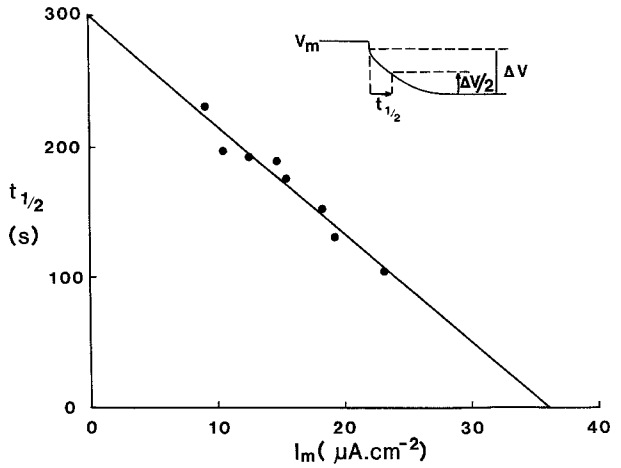

Fig. 5. The halftime ($t_{1/2}$) for slow potential changes to reach half their maximum value as illustrated in the inset. These values were obtained from the same fiber from the traces shown in Figs. 1, 3 and 4 together with an additional trace (not shown in those figures). It may be seen that $t_{1/2}$ decreases linearly as I_m increases, as predicted from the analysis given for transport number depletion of chloride (*see* text)

$$V_m = \frac{RT}{F} \ln \frac{[K]_o + \alpha[Na]_o + \beta[Cl]_i}{[K]_i + \alpha[Na]_i + \beta[Cl]_o} \tag{7}$$

from

$$[Cl]_i = (A_i \xi - A_o)/\beta \tag{8}$$

where

$$A_o \equiv [K]_o + \alpha[Na]_o \tag{9}$$

$$A_i \equiv [K]_i + \alpha[Na]_i + \beta[Cl]_o \tag{10}$$

and

$$\xi \equiv \exp(V_m F/RT) \tag{11}$$

where

$$\alpha \equiv P_{Na}/P_K \qquad \beta \equiv P_{Cl}/P_K. \tag{12}$$

P_{Na}/P_K and P_{Cl}/P_K were assumed to remain constant during and following the pulses.

A new value of $[Cl]_i$ was then calculated from $V(t_3)$, the immediate post-pulse potential, from

$$[Cl]_i = B_i \xi_2 + [Cl]_o \xi_2 - B_o \tag{13}$$

where

$$B_o \equiv ([K]_o + \alpha[Na]_o)/\beta \tag{14}$$

$$B_i \equiv ([K]_i + \alpha[Na]_i)/\beta \tag{15}$$

and

$$\xi_2 \equiv \exp(V(t_3) F/RT). \tag{16}$$

Although the absolute value of the chloride concentration following such current pulses is

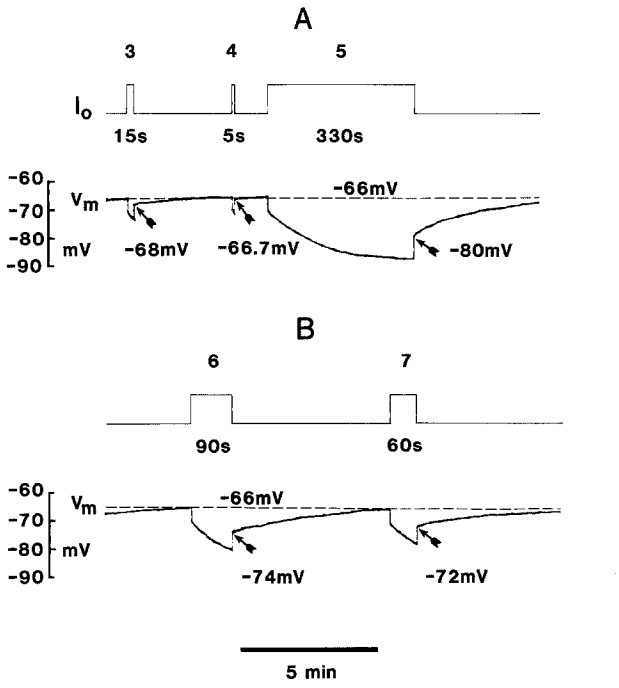

Fig. 6. Slow potential changes observed in the same mammalian muscle fiber for hyperpolarizing current pulses in a standard chloride solution (Solution *B* of Table 1). Although of the same magnitude, different length pulses were chosen to investigate the time course of chloride depletion within the fiber, as inferred from the immediate post-pulse potential ($V(t_3)$ in Fig. 7). *B* is a continuation of *A*. The top trace in each panel represents the total current I_o injected into the fiber and the bottom trace the membrane potential measured at V_1. It was very important that the initial resting membrane potential just before each current pulse was as close as possible (here $=-66$ mV) so as to reproduce close to identical starting conditions for each of the pulses. The values of the immediate post-pulse potentials indicated by the arrows were obtained directly from enlargements of the original records and were used in the calculations for Fig. 7. For this fiber, $T=17.6$ °C; the two electrode distances were 300 and 400 μm and $\delta\ell=100$ μm; the space constant, $\lambda=0.54$ mm; the fiber radius, $a=43$ μm and the current density in each case was 19.0 μA · cm^{-2}

dependent on the initial value of $[Cl]_i$, which is itself somewhat dependent on the value of P_{Na}/P_K chosen, the reduction in chloride concentration ($\Delta[Cl]_i = C(0) - C(t)$, where t is the pulse length) is virtually independent of this value. For the fiber in Fig. 6, for example, varying P_{Na}/P_K from 0.008 to 0.08 changes $C(0)$ the initial value of $[Cl]_i$ from 12.3 to 10 mM, which consequently only changes $\Delta[Cl]_i$ after a 330-sec pulse from 5.70 to 5.73 mM. A maximum value of $[Cl]_i = 12.4$ for the above fiber occurs if $P_{Na}/P_K = 0$. Secondly, the decrease in chloride concentration, $C(0) - C(t)$, is not critically dependent on P_{Cl}/P_K and changing it from 3.0 to 6.0 only changes $C(0) - C(t)$ from 6.2 to 5.4 mM for long 330-sec pulses (Table 2). Using the value of $P_{Na}/P_K = 0.008$ (Dulhunty, 1978), which yields $[Cl]_i = 12.3$, Eqs. (7)-(16) were used to calculate the values of $C(0) - C(t)$ given in Table 3. It may be seen that they tend to asymptote to a certain value as t increases. With a small offset adjustment (0.23 mM) to C(330 sec) to estimate the asymptotic value ($C(\infty)$) and allow for the fact that the concentration change after the 330-sec pulse had not quite reached a steady level, $C(t) - C(\infty)$ was well fitted by an exponential curve as indicated in Fig. 7, indicating that it is well described by the relationship

$$C(t) - C(\infty) = [C(0) - C(\infty)]\, e^{-t/\tau} \qquad (17)$$

where the time constant τ for the decrease in internal chloride is 92 sec.

Table 2. The dependence of the calculated initial concentration of chloride $C(0)$ and the decrease in concentration ($C(0) - C(t)$) at the end of a long pulse (pulse 5 in Fig. 6) on the value of $\beta(=P_{Cl}/P_K)$

$\beta(=P_{Cl}/P_K)$	2.0	3.0	4.5	6.0
$C(0)$	14.1	13.0	12.3	11.9
$C(0) - C(t)$[a] in mM	7.0	6.2	5.7	5.4

[a] $\alpha(=P_{Na}/P_K)$ was taken as 0.008, but as noted $C(0) - C(t)$ is essentially independent of $C(0)$. The pulse length was 330 sec (*See* Table 3, Fig. 6, and text for further discussion.)

Table 3. Changes in potential and calculated values of decrease in internal chloride concentration following a series of equal constant current pulses of differing duration[a]

Pulse No.	Pulse length (sec)	$V_m(t_3)$ (mV)	$C(0) - C(t)$[b] (mM)	$C(t) - C(\infty)$[c] mM
3	15	−68	1.022	4.91
4	5	−66.7	0.367	5.56
5	330	−80	5.70	0.23
6	90	−74	3.64	2.29
7	60	−72	2.84	3.09

[a] For further details about fiber parameters and experimental conditions *see* legend to Fig. 6.

[b] $C(0)$ the concentration inside the cell at the beginning of the pulse was taken as 12.3 mM. These values were calculated using Eqs. (7)-(16) by the procedure described in the text.

[c] $C(0)$ was taken as 12.3 mM and $C(O) - C(\infty) = 5.93$ mM.

Theoretical Analysis

So far we have shown that the large time-dependent hyperpolarization following long cur-

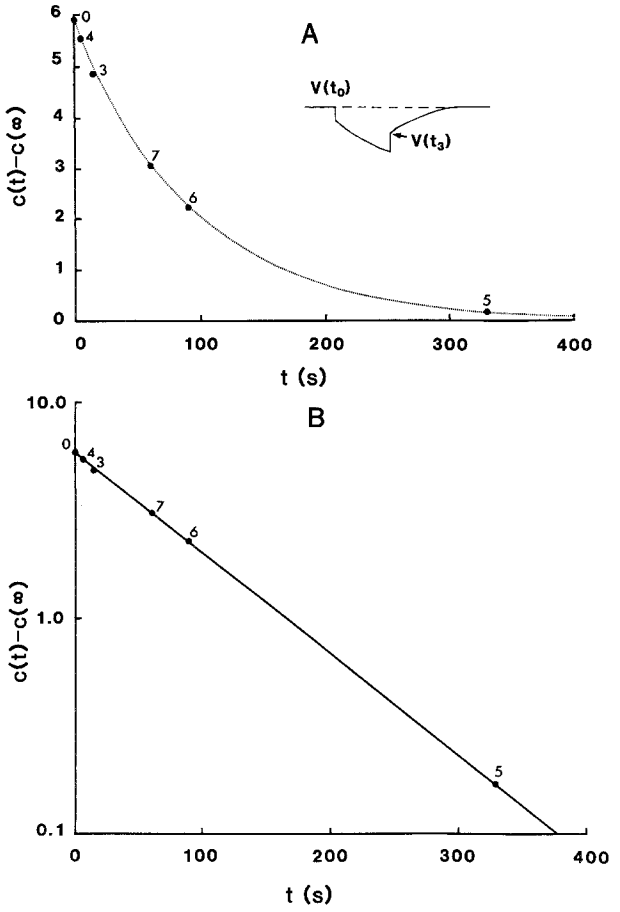

Fig. 7. Calculated values of chloride depletion following hyperpolarizing current pulses obtained from measurements of the immediate post-pulse potentials, as indicated by $V(t_3)$ in the inset to *A*), given in Fig. 6 and Table 3. The values of $C(0)-C(t)$ were obtained using Eqs. (7)–(16), with $C(0)=12.3$ mM evaluated from the resting potential of -66 mV with $P_{Na}/P_K=0.008$ and $P_{Cl}/P_K=4.5$. Thus $C(330\,\text{sec})=6.6$ mM. With a small adjustment to the asymptotic value $C(\infty)$ (so that $C(\infty)=6.37$ mM), $C(t)-C(\infty)$ was well fitted by a straight line as a function of t in the semi-logarithmic plot of *B*. *A* shows the exponential nature of this curve in a linear plot. In both panels the numbers 1–5 beside the experimental points (solid circles) refer to the time sequence of the pulses (*see* Fig. 6) and the "0" value refers to $C(0)-C(\infty)=5.93$ mM. Thus the relationship between concentration depletion and time t is given by Eq. (17) where from *B*, $\tau=92$ sec. This exponential relationship is also predicted from an analysis of transport number depletion effects in these fibers

rent pulses in mammalian muscle can be well explained in terms of a decrease in internal chloride concentration within the fiber. In this section we investigate the electrical basis for this and whether it can be quantitatively explained in terms of the expected response to such current pulses.

It is now well known that when currents are passed across membranes differences between the fraction of the current carried by a particular ion, i.e., differences between transport numbers in the membranes and in the solutions, will give rise to depletion and enhancement of salt in the unstirred regions adjacent to the membranes. This effect, which will be referred to here as the "transport number effect" (e.g., Barry & Hope, 1969), is also sometimes referred to as "concentration polarization" (e.g., Dewhurst, 1960). For a review of such effects, their mechanisms, and implications *see* either the specific review of transport number effects by Barry (1983) or the general review of unstirred-layer phenomena by Barry and Diamond (1984). The inside of the muscle fibers acts like an unstirred region, but there should also be an unstirred layer around the outside of the fibre. When a hyperpolarizing current is passed across the muscle membrane the low inside chloride concentration is depleted, with some limited compensation by chloride ions, which diffuse longitudinally from much further down the fiber. In contrast, the high external chloride concentration is enhanced and the increase in concentration is opposed by diffusion into the bulk solution beyond the external unstirred layer. Chloride will also accumulate in the unstirred region of the transverse tubules because of the high chloride permeability of the mammalian transverse tubular membrane (Dulhunty, 1979). However, diffusion of ions from the transverse tubules to the bulk solution occurs with a time course of seconds (Barry & Adrian, 1973) and is fast compared with the slow potential changes described here. Therefore, by far the most significant concentration change will take place within the fiber. The basic principles of the transport number effect are illustrated in Fig. 8. The transport number for ion i in free solution is given by

$$t_i=\frac{z_i u_i C_i}{\sum_j z_j u_j C_j} \tag{18}$$

where z_i, u_i and C_i are the valency, mobility, and concentration of ion i and the summation on the denominator is over all the j ions contributing to the current. Hence, since $u_{Cl}\cong u_K$ in free solution, within the internal 3 M KCl electrode $t_{Cl}\cong t_K\cong 0.5$ from Eq. (18). For the purpose of illustrating the effect, assume that the transport number of chloride in the membrane at a particular time during the pulse $t_{Cl}\cong 0.7$ so that the transport number of potassium $t_K\cong 0.3$.

Consider one Faraday of charge transferred

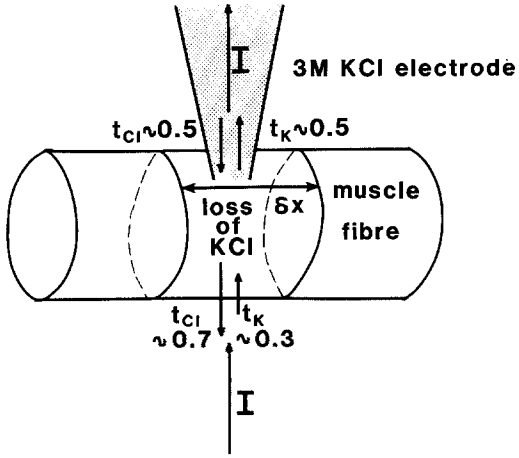

Fig. 8. A schematic diagram illustrating how depletion of chloride ions within a mammalian muscle fiber necessarily follows during hyperpolarizing pulses of current I. This automatically occurs providing the transport number of chloride (or fraction of current carried by chloride ions) in the membrane is greater than 0.5, its value in the 3 M KCl current electrode. For example, if its value at some time in the membrane is 0.7, for the passage of one Faraday of charge 0.5 moles of chloride will enter the fiber and 0.7 moles will leave, thereby depleting the fiber by 0.2 moles of chloride ions. Similarly 0.3 moles of potassium enters and 0.5 moles of potassium leaves, thereby depleting the fiber by 0.2 moles of potassium ions, so that overall the cell is depleted by 0.2 moles of potassium chloride, electroneutrality, of course, being automatically conserved. δx represents a length of fiber of radius a (used in the Appendix in order to calculated the surface/volume ratio in which chloride depletion occurs, the δx actually cancelling out). As indicated in the next two sections of the paper, the positioning of the current electrode, is, in reality, at some distance along the fiber from the voltage recording electrode V_1 (*see* Fig. 9*A*). Provided, however, that local chloride concentration equilibration within the fiber due to diffusion and local current effects is reasonably fast compared to the pulse length, this should not significantly affect any of the analysis

for current passed from the external solution into the fiber and thence into the internal microelectrode. Within the fiber 0.7 mole of chloride ions will be leaving across the fiber membrane and 0.5 mole will be arriving from the electrode. This means that 0.2 mole of chloride ions will be depleted from the fiber. Similarly 0.2 mole of potassium ions will likewise be lost, thereby resulting in a total depletion of 0.2 mole of potassium chloride. In the external solution where $t_{Cl}<0.7$ there will be an enhancement of potassium chloride. For a current I_m the actual rate of depletion of chloride from within the fiber, dn/dt, in moles $\cdot$ cm^{-2} (surface area) $\cdot$ sec^{-1} will be given by

$$\frac{dn}{dt}=\frac{(t^m_{Cl}-t^e_{Cl})}{F}I_m \tag{19}$$

where superscripts m and e refer to transport number values in the membrane and electrode, respectively, and F is the Faraday.

In the external unstirred solution layer the transport number perturbation of the local ion concentrations is balanced by diffusion down the concentration gradients set up between the membrane interface and the bulk solution. Within the fiber, chloride depletion should be taking place fairly equally within the whole closed-end of fiber region and to a more limited extent for a distance of about one space constant or so on the other side of the current electrode. Some diffusion of chloride could take place from beyond this region towards the depleted end but it is unlikely to be very significant and would be fairly slow (taking many minutes), whereas within the fiber, radial equilibration would be very fast (taking about a second). Chloride depletion could also tend to be balanced by both passive diffusion and active transport of chloride back across the muscle membrane. For the purpose of the following analysis, however, we will assume that such passive and active transport may be neglected below 24 °C, at least during the onset of the pulses.

Consider an elementary region of fiber of length δx, surface area δA and volume δV (assuming for the purposes of this discussion and consistent with the calculation of I_m from cable properties, that the fiber behaves as a simple uninvaginated cylinder) with fractional volume f_v of the fiber accessible to chloride. The rate of change of chloride concentration with time dC/dt will then be given, from Eq. (19) and Eqs. (A1)-(A3) of the Appendix, by

$$\frac{dC}{dt}=\frac{(t^m_{Cl}-t^e_{Cl})I_m\delta A}{Ff_v\delta V}=(t^m_{Cl}-t^e_{Cl})\frac{2I_m}{aFf_v}. \tag{20}$$

If $(t^m_{Cl}-t^e_{Cl})$ were to remain constant we would expect the internal chloride concentration to decrease linearly until chloride ions were completely depleted from within the fiber. However, the "chloride current" is moving out of the fiber and, in fact, will be proportional to the internal chloride concentration. t^m_{Cl} should then decrease from a high initial value until it eventually becomes equal to t^e_{Cl} and $dC/dt=0$ so that thereafter chloride depletion ceases. Provided the time-dependent shift in potential during the current pulse is mainly due to a shift in the diffusion potential component, which itself essentially reflects a shift in the chloride equilib-

rium potential, the driving force on chloride ions may be expected to remain constant (*see* Appendix for further discussion). If this were true then the chloride current would be essentially independent of any parameters other than $[Cl]_i$ during the current pulse and hence t^m_{Cl} could be approximated by

$$t^m_{Cl} = K\,C(t) \tag{21}$$

where $C(t)$ represents $[Cl]_i$ at time t after the onset of the current pulse and K is a constant of proportionality.

Making this assumption, it is shown in the Appendix that the depletion of chloride from within the fiber follows the following exponential relationship

$$C(t) - C(\infty) = [C(0) - C(\infty)]\, e^{-t/\tau} \tag{22}$$

where the time constant for chloride depletion τ is given by

$$\tau = \frac{a f_v F}{2 I_m K} \tag{23}$$

and where the final chloride concentration is given by

$$C(\infty) = t^e_{Cl}/K. \tag{24}$$

It should be noted that Eq. (22) is exactly the relationship obtained experimentally and plotted in Fig. 7, and this reinforces the validity of our assumptions about t^m_{Cl} as expressed in Eq. (21). It may be assumed that the initial value of t^m_{Cl} can be approximated for hyperpolarizing voltages by

$$t^m_{Cl} = \frac{G_{Cl}}{G_{Cl} + G_K} \cong \frac{P_{Cl}[Cl]_i}{P_{Cl}[Cl]_i + P_K[K]_o}. \tag{25}$$

Using a value of 4.5 for P_{Cl}/P_K and 12.3 mM for $[Cl]_i$ and 3.5 mM for $[K]_o$, $t^m_{Cl} = 0.94$. From Eq. (24) with $[Cl]_i = 12.3$ mM, $K = 0.94/12.3 = 0.0764\ \text{mM}^{-1} = 7.64 \times 10^4\ \text{cm}^3 \cdot \text{mol}^{-1}$ from Eq. (24) the final value of $[Cl]_i$, $C(\infty) = 6.5$ mM so that $C(0) - C(\infty) = 5.8$ mM very close to the experimentally extracted value of 5.9 mM. Using a reasonable value of 0.75 ± 0.05 for f_v the fraction of fiber volume accessible to ions such as chloride (A. Somlyo, *personal communication*), τ will be given from Eq. (23) by

$$\tau = \frac{43 \times 10^{-4} \times (0.75 \pm 0.05) \times 96{,}500}{2 \times 19 \times 10^{-6} \times 7.64 \times 10^4} = 107 \pm 7 \text{ sec}$$

which is also close to the experimentally extracted value of 92 sec for this fiber.

Furthermore, the simple inverse relationship between time constant and membrane current, expressed by Eq. (23), is exactly what was observed in Figs. 2 and 3, and plotted in Fig. 4 for $t_{1/2}$, which is linearly related to τ.

Transport Number Depletion or a Permeability Change?

Local concentration changes of electrolyte due to transport number differences between membranes and adjacent solutions are physicochemical effects that do always occur whenever currents are passed across cell membranes. The only question is one of magnitude. Can they explain the observed slow potential changes described in this paper without having to resort to alternative explanations such as that of a time-dependent and potential-dependent chloride permeability change. We have already shown that, provided estimates of P_{Cl}/P_K are reasonably accurate, the magnitude of transport number effects is sufficient to explain the observed slow potential changes. They also accurately predict the time course of these changes.

A careful analysis of the predicted $V_2 - V_1$ response during current pulses further supports the significant role of transport number effects and is at variance with a permeability mechanism. It should be pointed out that the earlier Fig. 8 is a slight oversimplification as far as the positioning of the current electrode is concerned, since that electrode is in reality close to V_2 and separated some distance down the fiber from V_1, where the potential is being recorded (*see* inset to Fig. 1). This means that strictly at the membrane near V_1 and current electrode the transport number differences are $(t^m_{Cl} - t^s_{Cl})$ and $(t^s_{Cl} - t^e_{Cl})$, respectively, where t^s_{Cl} is the chloride transport number in the sarcoplasm (~ 0.06). Initially the value of V_1 will be somewhat less than V_2 because of the cable properties of the fibers. Indeed for the fiber results shown in Fig. 9 *C*, V_1 should be just over half of V_2 with I_1 and I_2 being somewhat in proportion. The relative magnitudes of these currents will, however, be more than compensated for by different transport number differences near V_1 and V_2. The transport number of chloride at V_1 is expected to initially be about 0.9 so that $t^m_{Cl} - t^s_{Cl} \cong 0.89$ whereas at V_2 it will be given approximately by $t^m_{Cl} - t^e_{Cl} \cong 0.9 - 0.5 = 0.4$. For low-

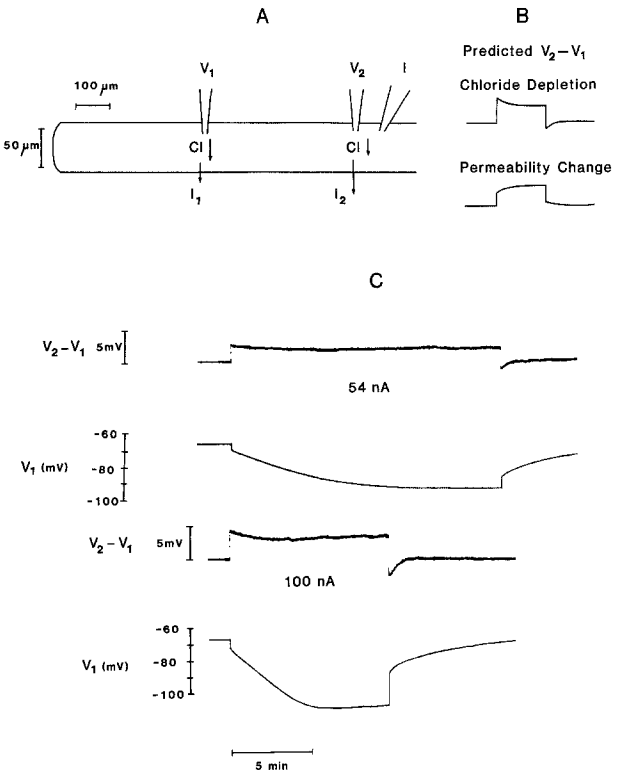

Fig. 9. Predictions of transport number depletion and permeability changes on the voltage difference V_2-V_1 between electrodes 1 and 2 on a three-electrode current-clamped muscle fiber compared with experimental records. *A* shows the experimental electrode placement, from which the records in *C* were obtained. For convenience, however, the scale of the fiber diameter in *A* has been doubled as indicated. For this fiber with a space constant of about 590 μm the initial value of V_1 should be just over half of V_2 because of the cable properties of the cell and the currents have been drawn in proportion. The transport number difference between the membrane at V_1 and the fiber interior would be more than twice the difference between the membrane at V_2 and the current electrode close by. In addition there would be more diffusion of Cl from the remainder of the fiber at V_2 and perhaps also from the current electrode. This would imply that Cl depletion would be greater around V_1 than at V_2. Also Cl would return to normal much faster at V_2 than at V_1. This picture predicts a V_2-V_1 response as illustrated in the top trace of *B*. In contrast, as indicated in the text, a permeability change mechanism would predict the response illustrated in the lower trace. This is because the current at V_2 should be greater than at V_1 and greater current should produce a greater permeability change with time (as would be supported by the two current responses in *C*), thus causing V_2-V_1 to increase with time as shown. *C* shows the typical response obtained with a 3 M KCl current electrode for the same fiber used for Figs. 1, 3 and 4. The response is very similar to the predictions of transport number depletion and quite different from those suggested by a permeability change

er values of t_{Cl}^m the transport number difference at V_2 becomes smaller still relative to that at V_1. In addition there would be more diffusion of KCl from the remainder of the fiber towards V_2 and perhaps even some from the current electrode. These effects imply that Cl depletion would be greater at V_1 than at V_2, thus causing V_2-V_1 to initially decrease with time. Eventually, such longitudinal concentration differences along the end region of the fiber would tend to equilibrate by both diffusion and local current effects and by the asymptotic "saturating" nature of the predicted transport number effects and V_2-V_1 would tend to flatten out. At the end of the pulse V_2 would recover much faster than V_1 because of diffusion and local current effects from the remainder of the fiber. Hence V_2-V_1 would initially tend to go negative. These results are exactly what we always recorded with a potassium chloride current electrode for fiber in a standard chloride bathing solution (e.g., Fig. 9 *C*; *see also* Fig 1).

In contrast, for a permeability mechanism, with the permeability increasing monotonically with the change in membrane potential and with time, a very different response would be expected. Since V_2 is greater than V_1, the permeability change at V_2 should also be greater. Thus V_2-V_1 would initially be expected to increase with time as indicated in the lower trace of Fig. 9 *B*. At the end of the pulse it pould be expected that the greater permeability change expected at V_2 would take longer to return to the resting value than V_1 and hence V_2-V_1 would appear as in the predicted trace. This response is not observed experimentally.

An obvious experiment to further distinguish between these two mechanisms would be to replace the electrolyte in the current electrode by a large relatively impermeant anion such as citrate. Any responses due to a permeability change mechanism should be independent of such electrolyte replacement in the current electrode. In contrast, with citrate in the current electrode, the transport number differences at V_1 and V_2 would now be very similar. Since I_2 is greater than I_1, because of the cable properties of the fiber, Cl depletion would now be initially greater at V_2 than V_1 so that V_2-V_1 would initially increase with time. At the end of a current pulse, however, because of the end-of-fiber setup Cl should diffuse towards V_2 from further down the fiber and hence V_2 should recover faster than V_1 so that V_2-V_1 should become more negative than the final baseline level. This voltage response, predicted by transport number depletion of Cl, is what was invariably observed in a series of experiments with chloride being replaced by citrate in the current electrode as illustrated for two different experiments in Fig. 10.

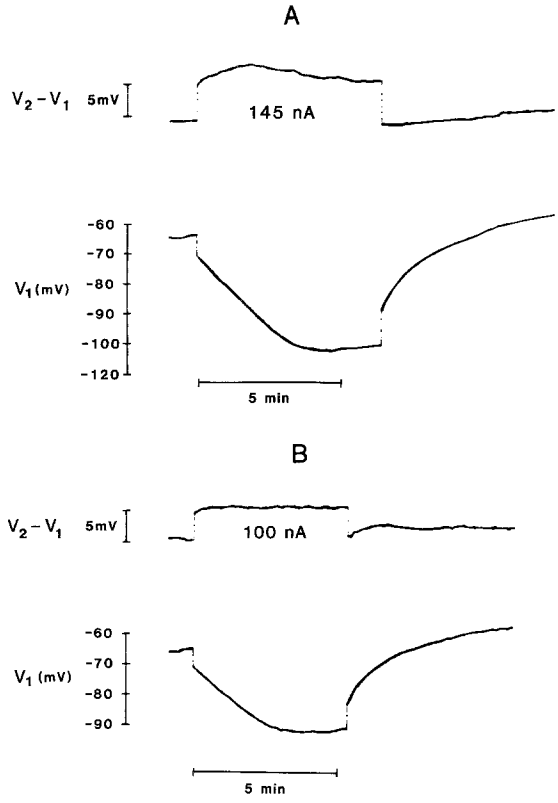

Fig. 10. Two sets of experimental records of slow potential changes at V_1 and the V_2-V_1 response using potassium citrate in the current electrode rather than potassium chloride. The conditions were essentially the same as for the other experiments reported (e.g., Fig. 9) and solution *D* (Table 1) was used. In *A* interelectrode distances ℓ and $\delta\ell$ were 500 and 60 μm, the calculated fiber radius a was 42 μm, current density I_m was 22 μA·cm^{-2}, membrane resistance $R_m=0.32$ kΩ cm^2, and temperature $T=22$ °C. *B* is a record from a different fiber in which $\ell=500$ μm, $\delta\ell=120$ μm, $a=38$ μm, $R_m=0.40$ kΩ cm^2 and $T=21.4$ °C. Both records in *A* and *B* were typical of those obtained with potassium citrate current electrodes and which contrasts with typical potassium chloride current electrode results (e.g., Fig. 9*C*). The V_2-V_1 response initially increases during the current pulse, reflecting a more rapid increase in the magnitude of V_2 than V_1. This difference, dependent on the current electrode electrolyte, is as predicted by transport number effects (*see* text). Nevertheless, V_2-V_1 still appears to go negative with respect to its final baseline level (most clearly seen in *A*), implying that V_2 recovers faster than V_1, again as predicted from transport number depletion effects.

It is thus clear that not only are all these results predicted by transport number depletion effects but some of them are in complete contrast with a permeability mechanism.

These slightly different transport number effects at V_1 and V_2 might explain the concentration depletion calculated for pulses 3 and 4 in Fig. 7 being very slightly below the fitted curve. They would also help to account for the slight difference between the estimated and measured values of the time constant.

Also at the end of the pulse, when the current is reduced to zero, the driving force on chloride will be very small and outward. For example, in the case considered in the Appendix, $F_{Cl}\cong(-80-(-78.6))=-1.4$ mV at the end of a 330-sec pulse. Therefore there will not be much of a passive influx of chloride immediately following the pulse. The slow repolarization must therefore be mainly due to longitudinal diffusion and local current flow from the non-chloride depleted region of the fiber together with a possible contribution from active transport of chloride back into the fiber.

Discussion

The results in this paper show that, in addition to the usual relatively fast time-dependent potential changes ("creep") observed in amphibian fibers during hyperpolarizing currents in low chloride solutions, mammalian fibers exhibit a very large and slow time-dependent potential change in standard chloride solutions so that the internal chloride concentration and chloride transport number in the membrane are reduced. This slower time-dependent increase in potential during the current pulse, is radically reduced by lowering the chloride concentration in the external solution.

Three possible explanations can be advanced to explain these results: (1) changes in chloride conductance (2) changes in P_{Cl}/P_K and (3) changes in $[Cl]_i$. While changes in chloride conductance might be able to explain the transient voltage response during the onset of the current, such changes in conductance cannot simply explain the intermediate hyperpolarizing levels, when the current is terminated, or the slow recovery back to the resting membrane potential. Similarly, changes in P_{Cl}/P_K would have to be very large, going from about 4.5 down to about 0.3 during the passage of the current pulse and would likewise have to have some complicated built-in delay mechanism to account for the hyperpolarized potential response *after* the current pulse. The third possibility is in a different category from the first two since it accurately predicts the slow creep in terms of known transport number effects, which by themselves will give rise to a depletion of chloride within the fiber, without having to invoke any additional unknown factors such as delayed changes in ionic permeabilities. The transport number of an ion is a measure of the fraction of current carried by that ion, and transport number effects occur

whenever there is a difference in transport numbers between a membrane and an adjacent solution. In the absence of perfect stirring within any unstirred layers or regions adjacent to a membrane, these transport number effects give rise to solute enhancement or depletion within these regions, which itself can result in a time-dependent diffusion potential component, which can mimic a capacitance and also produce electroosmotic flow (e.g., for review, *see* Barry, 1983).

In mammalian fibers it is to be expected that the predominant transport number effect during a hyperpolarizing current pulse will be depletion of chloride within the internal unstirred volume of the fibers. Because of the normally low internal concentration and high membrane conductance for chloride ions, the reduction in internal concentration should be reflected in a time-dependent hyperpolarization of the membrane potential, which would only slowly return to its resting level, as the internal concentration recovers following the termination of the pulses.

Using accepted values of P_{Cl}/P_K and P_{Na}/P_K and internal $[K]_i$ and $[Na]_i$, the internal concentration of chloride was calculated from the resting membrane potential using the Goldman-Hodgkin-Katz Equation, and values of 10–12 mM were obtained for fibers with potentials in the range from -70 to -66 mV. From the level of hyperpolarization immediately after a current pulse, final values of $[Cl]_i$ were calculated. For example, for one of the fibers with an initial $[Cl]_i$ of 12.3 mM, such calculations indicated that by the end of a 300-sec pulse the final $[Cl]_i$ had dropped to 6.6 mM. By extracting values of this final $[Cl]_i$ at the end of pulses of different lengths, it was shown that the chloride concentration decreased exponentially with time with a final asymptotic value of 6.4 mM and a time constant of 92 sec.

The assumption that the chloride current was essentially only proportional to the internal chloride concentration was validated since the driving force on chloride remained essentially constant throughout the current pulse. Using this assumption it was predicted that the internal chloride concentration should decrease exponentially during the current pulse. Such a predicated change in concentration was identical in form to that obtained experimentally. When measured values of the fiber parameters were used in the equations a final asymptotic value for internal chloride of 6.5 mM was obtained and this is very close to the experimentally extracted one of 6.4 mM. Likewise, the predicted time constant was 107 sec also close to that obtained experimentally (92 sec). Similarly, the predicted inverse relationship between the time constant of the slow potential changes and membrane current was exactly equivalent to what was observed experimentally with the relationship between the halftime of the creep and membrane current.

In addition, as we have already noted in the previous section, the $V_2 - V_1$ response with KCl current electrodes was predicted by transport number effects and the opposite of what was expected from a permeability mechanism. In further support, this $V_2 - V_1$ response changed as predicted for a transport number effect when chloride was replaced by citrate in the current electrode in contrast with the predictions of a permeability mechanism.

Presumably the recovery of the potential is slow because even just after the end of the pulse the driving force on chloride ions is still outward, as it was during the pulse itself (*see* Appendix), and very small (e.g., for the 330-sec pulse illustrated in Fig. 6, $E_{Cl} \cong -1.4$ mV). Therefore there will not be any passive influx of chloride across the surface membrane immediately after the pulse.

Thus repolarization of the potential back to the resting value after the pulse must be primarily due to a diffusion of chloride ions from the undepleted region of the fiber into the depleted end, aided by local current flow effects together with some active transport (expected to be somewhat minimal at these temperatures) of chloride back into the fiber from the external solution. The increased initial rate of recovery seen following fibers depleted with large current pulses (e.g., Fig. 4*C*) may reflect a greater rate of active transport turned on by the greater amount of chloride depletion over the whole end region of the fiber.

The slow transport number depletion effects not only simulate a transient increase in membrane resistance but will also mimic capacitance effects at very low frequencies (i.e., <0.01 Hz) somewhat analogous to the faster transport number depletion of potassium in the transverse tubular system of amphibian muscle (Barry, 1977).

Transport number effects occurring during the passage of current across other cell membranes may well also give rise to somewhat similar slow potential changes, which could be

mistaken for time- and voltage-dependent permeability changes.

We would like to acknowledge the support of the Australian Federal CPPER Grant, and the Australian Research Grants Scheme and the Muscular Dystrophy Association of America for the experiments and during the preparation of this paper. We would also like to express our appreciation to Elaine Bonnet and Cynthia Prescott for their help in its preparation and to Professor P.W. Gage and Drs. G.D. Lamb and R.E. Wachtel for their helpful comments.

References

Adrian, R.H., Chandler, W.K., Hodgkin, A.L. 1970. Voltage clamp experiments in striated muscle fibers. *J. Physiol. (London)* **208**:607–644

Adrian, R.H., Freygang, W.H. 1962. The potassium and chloride conductance of frog muscle membrane. *J. Physiol. (London)* **163**:61–103

Almers, W. 1972*a*. Potassium conductance changes in skeletal muscle and the potassium concentration in the transverse tubules. *J. Physiol. (London)* **225**:33–56

Almers, W. 1972*b*. The decline of potassium permeability during extreme hyperpolarization in frog skeletal muscle. *J. Physiol. (London)* **225**:57–83

Barry, P.H. 1977. Transport number effects in the transverse tubular system and their implications for low frequency impedance measurement of capacitance of skeletal muscle fibers. *J. Membrane Biol.* **34**:383–408

Barry, P.H. 1983. Effects of unstirred-layers on the movement of ions across cell membranes. *Proc. Aust. Physiol. Pharmacol. Soc.* **14**:152–169

Barry, P.H., Adrian, R.H. 1973. Slow conductance changes due to potassium depletion in the transverse tubules of frog muscle fibers during hyperpolarizing pulses. *J. Membrane Biol.* **14**:243–292

Barry, P.H., Diamond, J.M. 1984. Effects of unstirred layers on membrane phenomena. *Physiol. Rev. (in press)*

Barry, P.H., Dulhunty, A.F. 1983. Slow conductance changes in mammalian muscle fibers during prolonged hyperpolarization. *Proc. Aust. Physiol. Pharmacol. Soc.* **14**:41*P*

Barry, P.H., Hope, A.B. 1969. Electroosmosis in membranes: Effects of unstirred layers and transport numbers. I. Theory. *Biophys. J.* **9**:700–728

Davey, D.F., Dulhunty, A.F., Fatkin, D. 1980. Glycerol treatment in mammalian skeletal muscle. *J. Membrane. Biol.* **53**:223–233

Dewhurst, D.J. 1960. Concentration polarization in plane membrane-solution systems. *Trans. Faraday Soc.* **56**:599–609

Dulhunty, A.F. 1978. The dependence of membrane potential on extracellular chloride concentration in mammalian skeletal muscle fibers. *J. Physiol. (London)* **276**:67–82

Dulhunty, A.F. 1979. Distribution of potassium and chloride permeability over the surface and T-tubule membranes of mammalian skeletal muscle. *J. Membrane Biol.* **45**:293–310

Eisenberg, R.S., Gage, P.W. 1969. Ionic conductances of the surface and transverse tubular system in frog sartorious fibers. *J. Gen. Physiol.* **53**:279–297

Goldman, D. 1943. Potential impedance and rectification in membrane. *J. Gen. Physiol.* **27**:37–60

Hodgkin, A.L., Katz, B. 1949. The effects of sodium ions on the electrical activity of the giant axon of the squid. *J. Physiol. (London)* **108**:37–77

Hodgkin, A.L., Nakajima, S. 1972. Effect of diameter on the electrical constants of frog skeletal muscle fibers. *J. Physiol. (London)* **221**:105–120

Lipicky, R.J., Bryant, S.H. 1966. Sodium, potassium, and chloride fluxes in intercostal muscle from normal goats and goats with hereditary myotonis. *J. Gen. Physiol.* **50**:89–111

Palade, P.T., Barchi, R.I. 1977. Characteristics of chloride conductance in muscle fibers of rat diaphragm. *J. Gen. Physiol.* **69**:325–342

Received 21 July 1983; revised 31 October 1983

Appendix

Transport Number Depletion of chloride from the Inside of a Cylindrical Fiber

Consider an elementary region of fiber of length δx, surface area δA and volume δV. If the fiber radius is a, then

$$\delta A = 2\pi a \delta x \tag{A1}$$

$$\delta V = \pi a^2 \delta x \tag{A2}$$

$$\delta \mathrm{A}/\delta \mathrm{V} = 2/\mathrm{a}. \tag{A3}$$

Assumption: During a constant current pulse the transport number for chloride ions in the membrane t^m_{Cl} will be given by

$$t^m_{\mathrm{Cl}} = K\,C(t) \tag{A4}$$

where $C(t)$ represents the internal chloride concentration at time t after the onset of the current pulse and K is a constant of proportionality. This is not too unreasonable, since the outward moving 'chloride current' is proportional to the internal chloride concentration and the total current is kept constant and will remain constant provided the driving force on chloride remains constant.

The loss of chloride ions during a constant current pulse of magnitude I_m amp$\cdot$cm^{-2} in moles dn in time dt will be given by

$$dn = -(t^m_{\mathrm{Cl}} - t^e_{\mathrm{Cl}})\,\delta A\, I_m\, dt/F \tag{A5}$$

where t^e_{Cl} is the transport number for chloride ions in the current electrode (normally $\cong 0.5$ since 3 M KCl electrodes were used). The concentration change in volume δV in time dt will then be given from Eqs. (A4) and (A5) by

$$dC = -(KC - t^e_{\mathrm{Cl}})\frac{\delta A}{\delta V}\frac{I_m}{f_v F}\,dt \tag{A6}$$

where f_v represents the fractional volume of the fiber accessible to chloride. Thus

$$\frac{dC}{dt} = -BC + D \tag{A7}$$

where B and D are defined by

$$B \equiv \frac{2I_m K}{af_v F} \tag{A8}$$

$$D \equiv \frac{2}{a}\frac{I_m t^e_{Cl}}{f_v F}. \tag{A9}$$

The full solution of Eq. (A7) can very readily be shown to be

$$C(t) = \frac{D}{B} + Ae^{-Bt} = \frac{t^e_{Cl}}{K} + Ae^{-Bt} \tag{A10}$$

where A is a constant of integration. Substituting the values for $C(t)$ when $t=0$ and $t=\infty$ to evaluate A and expressing $\tau \equiv 1/B$ we obtain

$$C(t) - C(\infty) = [C(0) - C(\infty)]e^{-t/\tau} \tag{A11}$$

where

$$\tau = \frac{af_v F}{2I_m K} \tag{A12}$$

and where

$$C(\infty) = t^e_{Cl}/K = t^e_{Cl}\, C(0)/t^m_{Cl}(0) \tag{A13}$$

where $t^m_{Cl}(0)$ is the value of t^m_{Cl} at the beginning of the pulse. As far as the assumption about the constancy of the driving force on chloride is concerned consider, for example, pulse 5 in Fig. 6. V_m at the beginning and end of the potential change (during the current pulse) is -70 and -86 mV, respectively. Assuming that the driving force F_{Cl} on chloride ions may be approximated by

$$F_{Cl} = V_m - \varepsilon_{Cl} = V_m + \frac{RT}{F}\ln\frac{[Cl]_o}{[Cl]_i}. \tag{A14}$$

At the beginning of the time-dependent part of the pulse (assuming $[Cl]_i = 12.3$ mM) $F_{Cl} = -70-(-62.7) = -7.3$ mV, whereas at the end of the pulse $F_{Cl} = -86-(-78.6) = -7.6$ mV, where from Table 2, $[Cl]_i = 12.3 - 5.7 = 6.6$ mM.